Electronic Supplementary Material (ESI) for Energy & Environmental Science.

Regulated Lithium Plating and Stripping by a Nano-Scale Gradient Inorganic-Organic Coating for Stable Lithium Metal Anodes

Yipeng Sun[1, 2], Changtai Zhao[1], Keegan R. Adair[1], Yang Zhao[1], Lyudmila V. Goncharova[3], Jianneng Liang[1], Changhong Wang[1], Junjie Li[1], Ruying Li[1], Mei Cai[4]*, Tsun-Kong Sham[2]*, Xueliang Sun[1]*

[1] Department of Mechanical and Materials Engineering
University of Western Ontario, London, Ontario, N6A 5B9, Canada
E-mail: xsun@eng.uwo.ca (X.L. Sun)

[2] Department of Chemistry
University of Western Ontario, London, Ontario, N6A 5B7, Canada
E-mail: tsham@uwo.ca (T.K. Sham)

[3] Department of Physics and Astronomy
University of Western Ontario, London, Ontario, N6A 3K7, Canada

[4] General Motors R&D Center
Warren, MI 48090-9055, USA
E-mail: mei.cai@gm.com

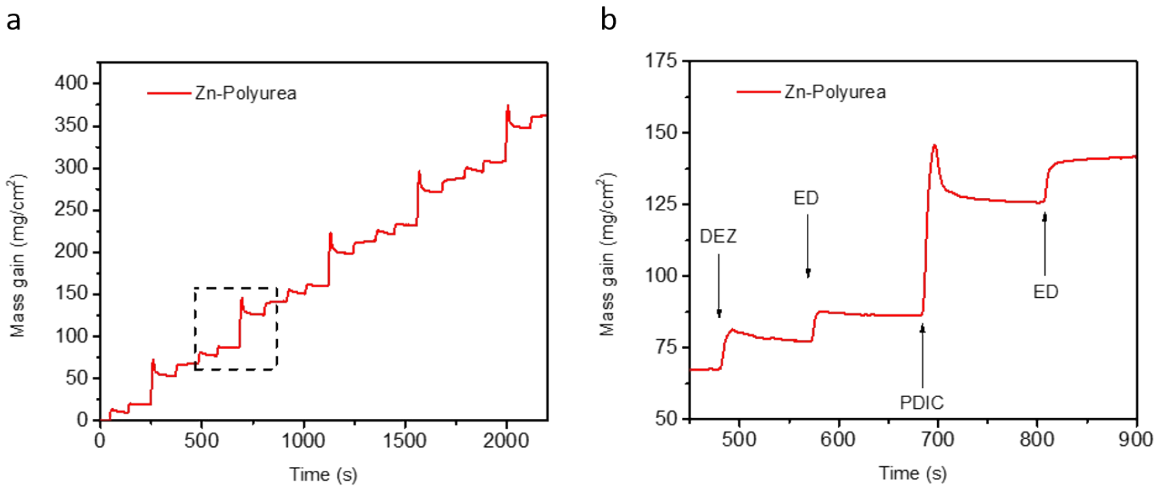

Figure S1. (a) The film growth of MLD Zinc-polyurea coating monitored by quartz crystal microbalance (QCM). (b) Detailed spectrum of a full MLD cycle.

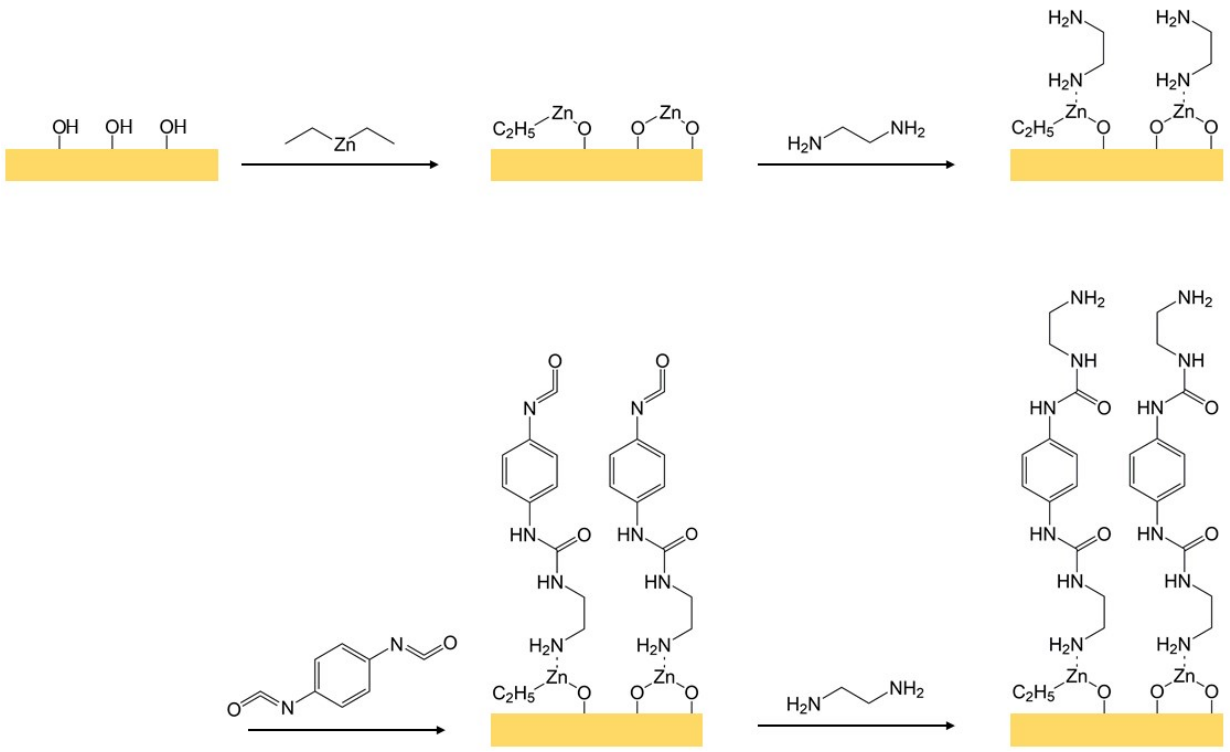

Figure S2. An illustration for a single MLD cycle of Zn-polyurea coating.

Firstly, DEZ reacts with the surface hydroxyl groups on the substrate and the side product of ethane is purged away. Secondly, ED is introduced to coordinatively react with the Zn center and expose an amine end group. Next, PDIC is pulsed into the surface and form urea bond without generating any gaseous side product. Finally, another pulse of ED forms another urea bond by the chemical reaction between -NCO group and -NH_2 group.

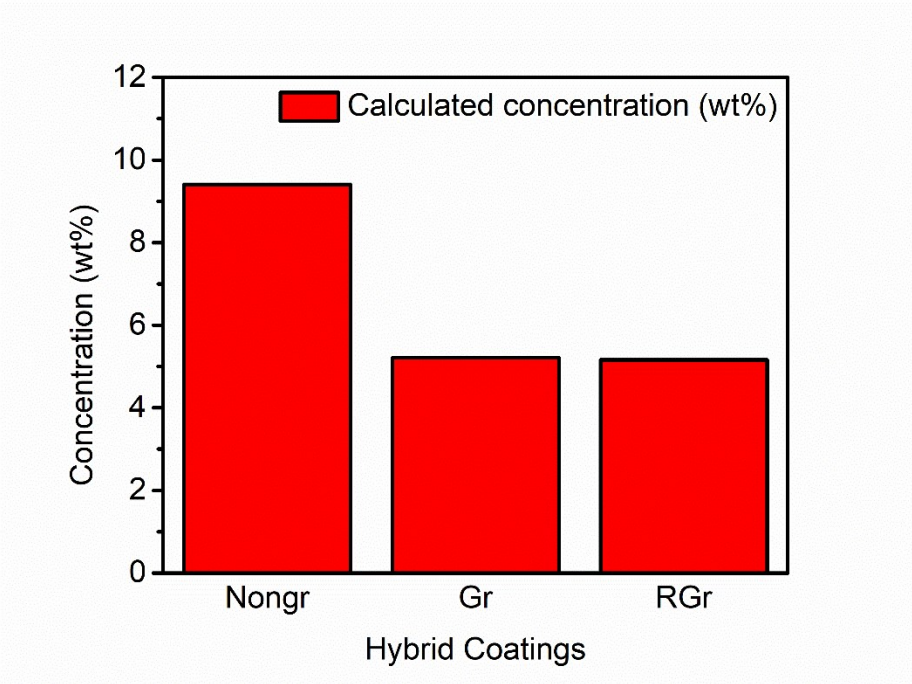

Figure S3. ICP results showing the relative Zn concentration of non-gradient, gradient and reversed gradient MLD coatings.

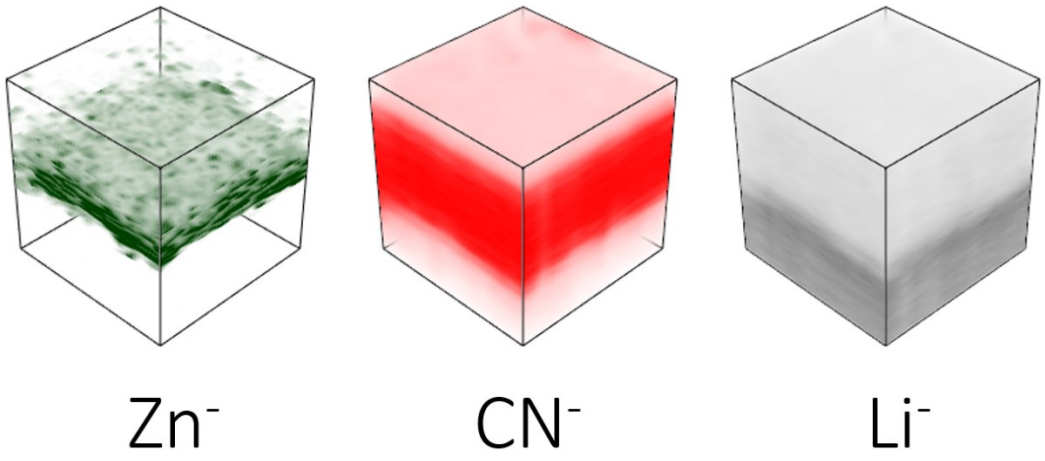

Figure S4. 3D reconstruction of secondary ions from TOF-SIMS depth profile for Zn^-, CN^-, and Li^-.

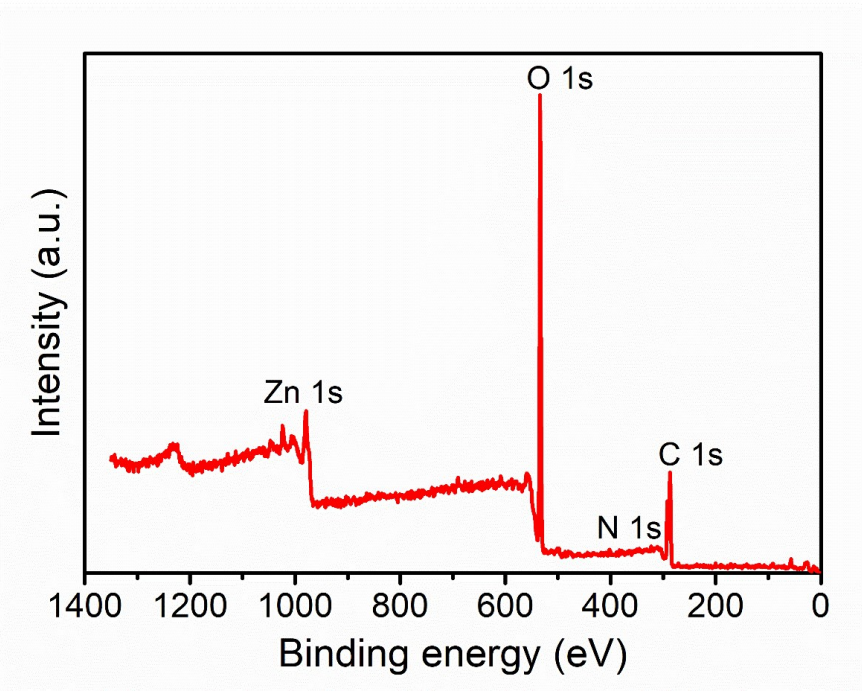

Figure S5. XPS survey spectrum of Li@Gr10.

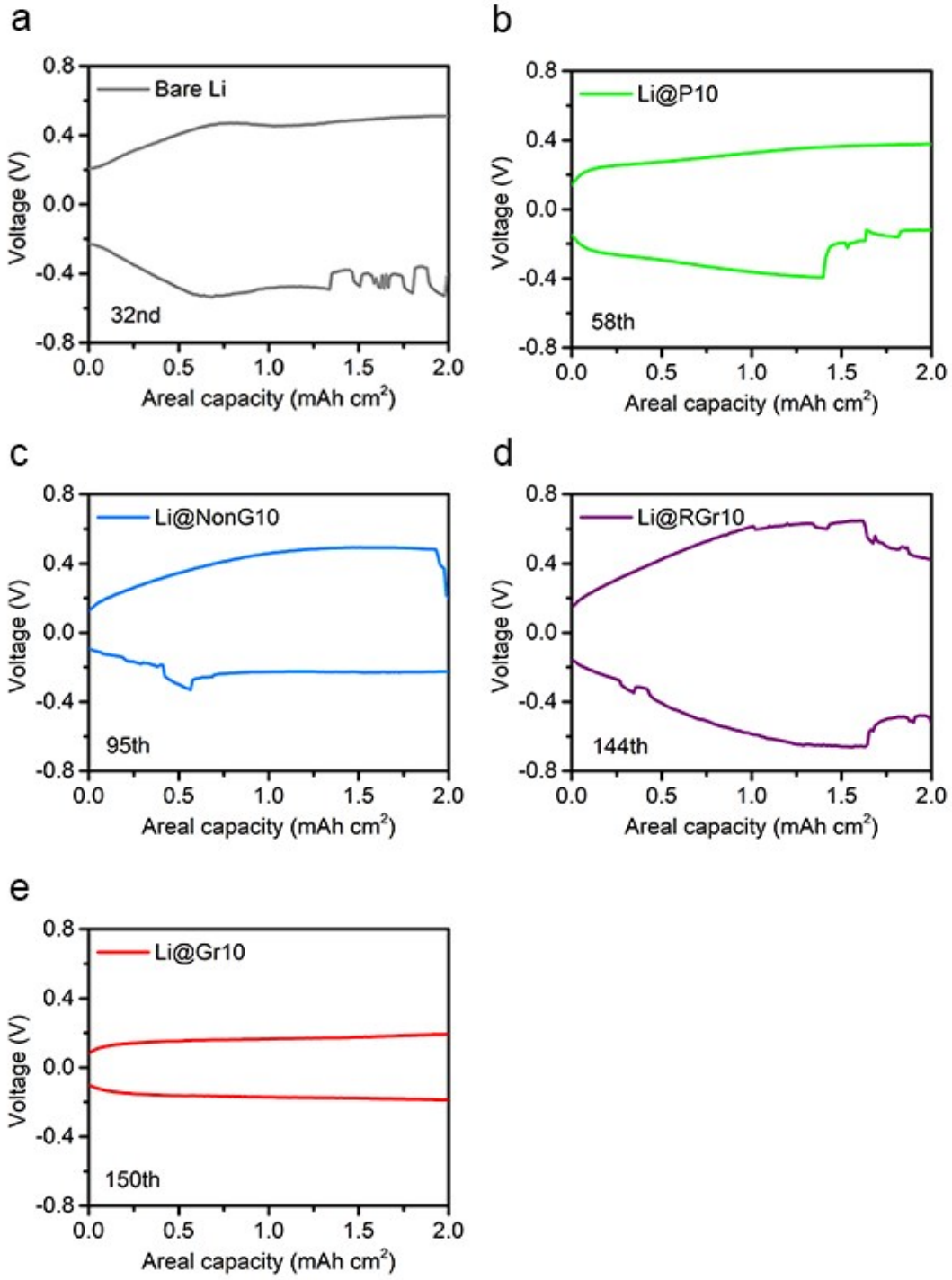

Figure S6. Detailed voltage profiles for bare Li and various MLD coated Li to track the happening time of short-circuiting that cycled at a current density of 4 mA cm^{-2}. (a) 32nd cycle for bare Li. (b) 58th cycle for Li@P10 (c) 95th cycle for Li@NonG10 (d) 144th cycle for Li@RGr10 (e) 150th cycle for Li@Gr10.

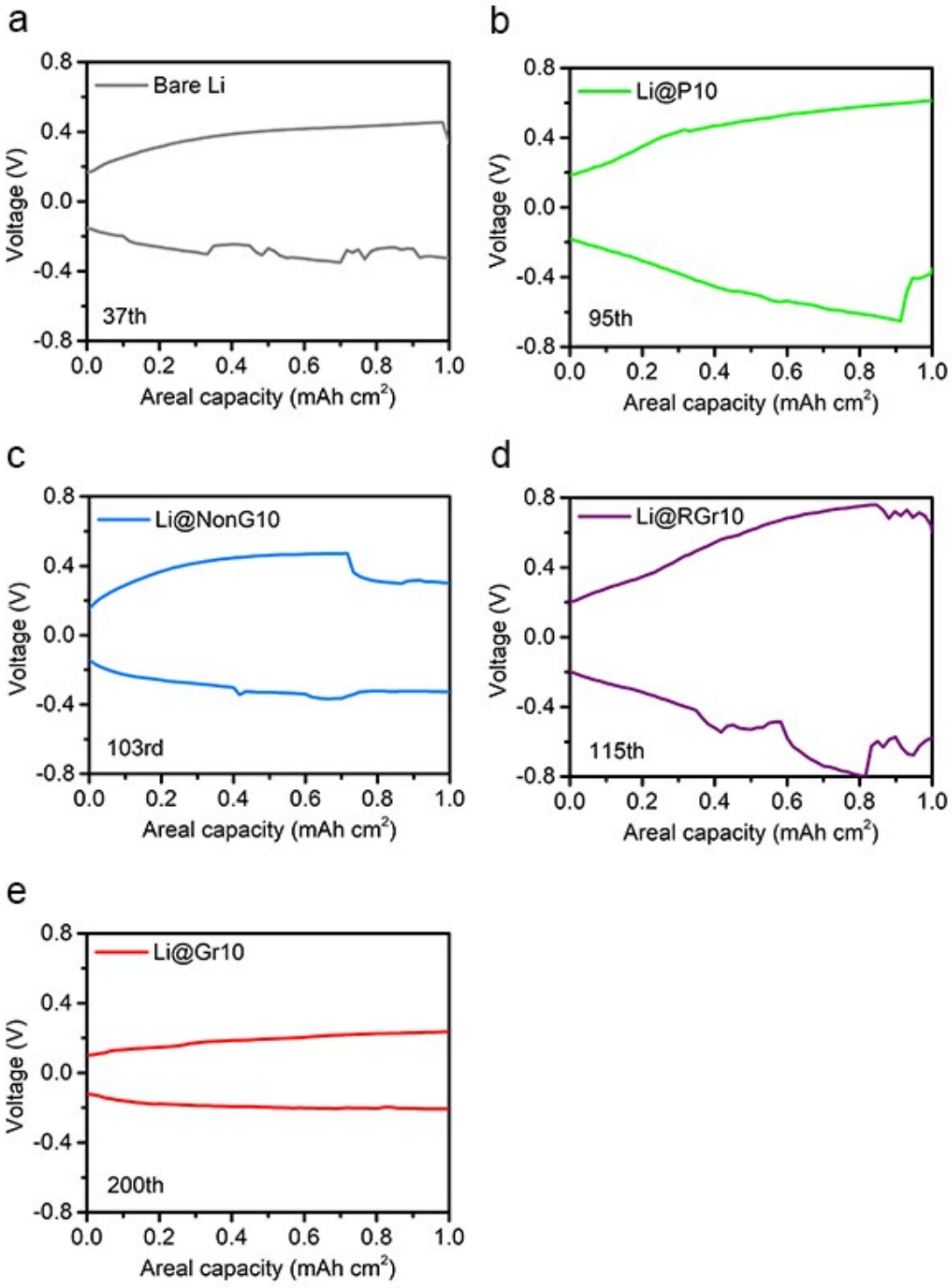

Figure S7. Detailed voltage profiles for bare Li and various MLD coated Li to track the happening time of short-circuiting that cycled at a current density of 6 mA cm^{-2}. (a) 37th cycle for bare Li. (b) 95th cycle for Li@P10 (c) 103rd cycle for Li@NonG10 (d) 115th cycle for Li@RGr10 (e) 200th cycle for Li@Gr10.

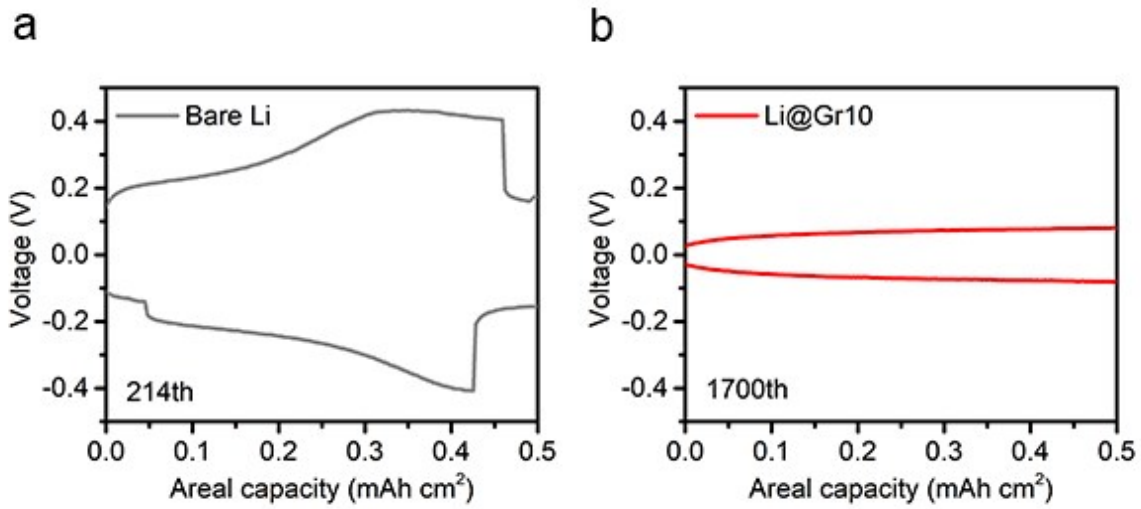

Figure S8. Detailed voltage profiles for both bare Li and Li@Gr10 that cycled at a current density of 1 mA cm^{-2}. (a) 214^{th} cycle for bare Li. (b) 1700^{th} cycle for Li@Gr10

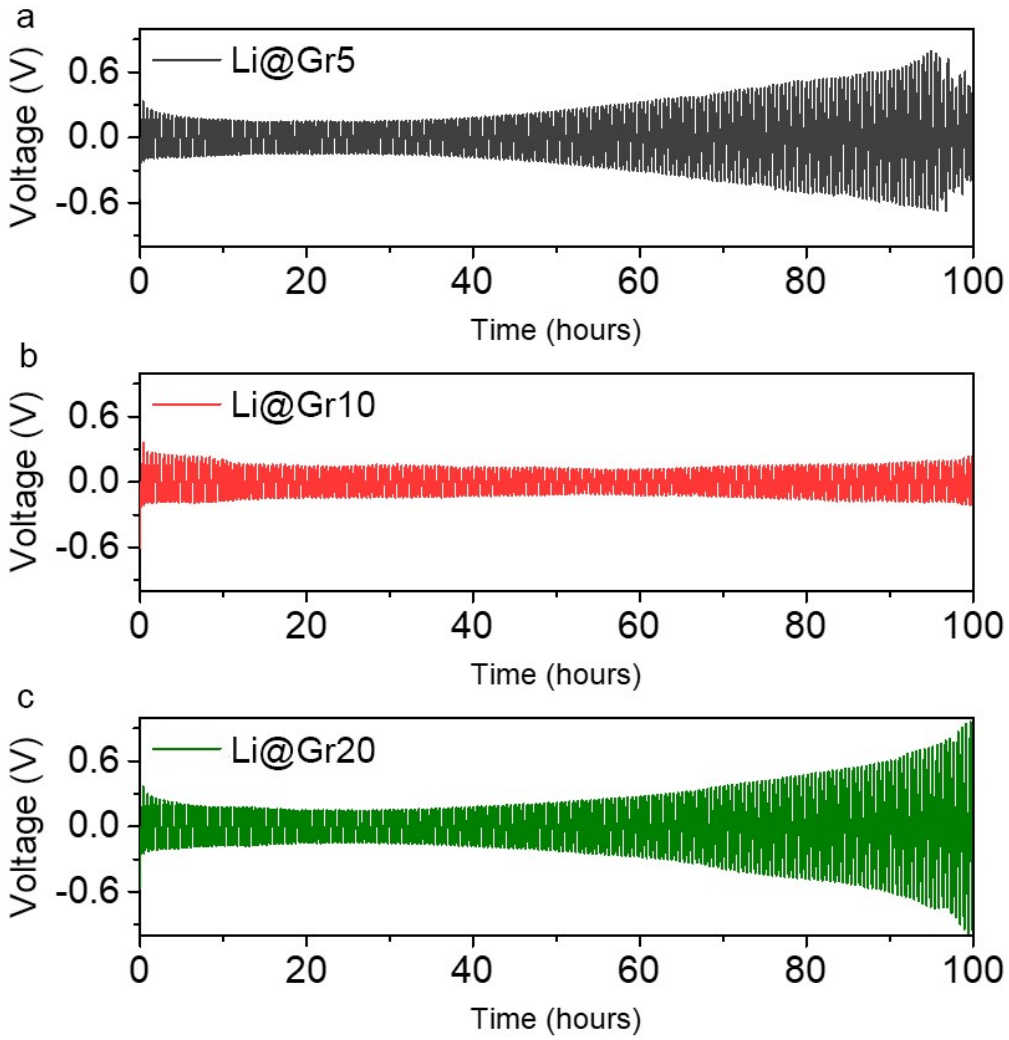

Figure S9. Voltage profile of (a) Li@Gr5, (b) Li@Gr10, and (c) Li@Gr20 in symmetric cells cycling at a current density of 6 mA cm^{-2}.

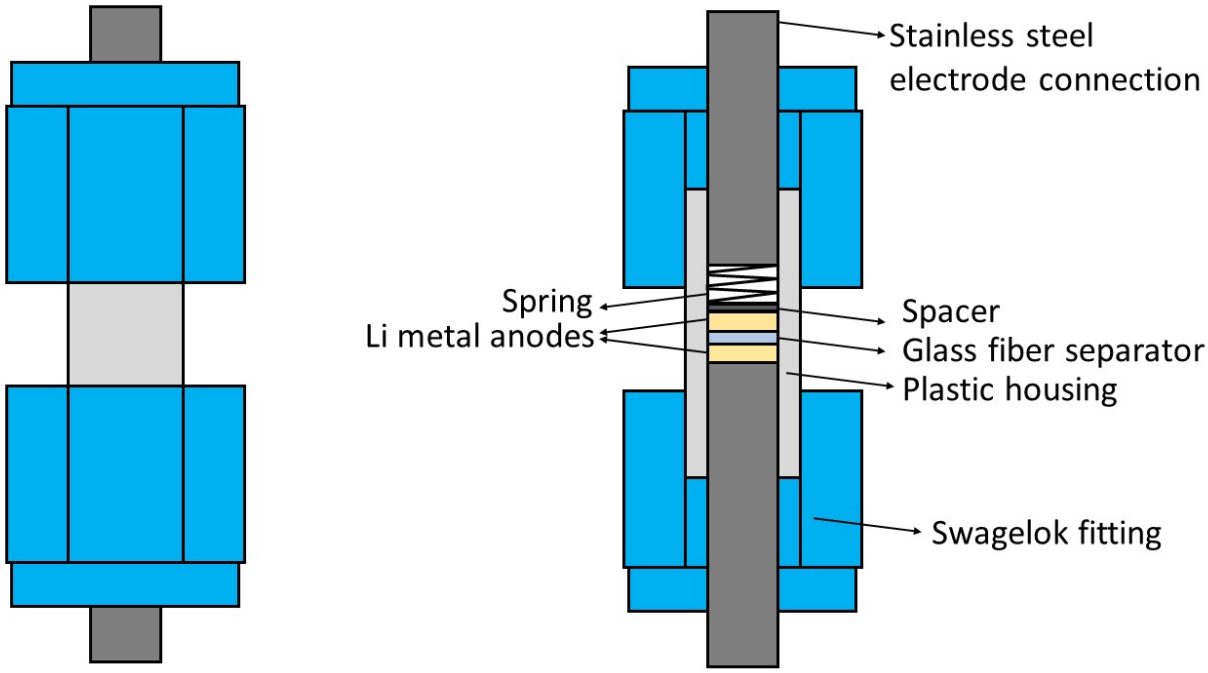

Figure S10. Schematic diagram of the Swagelok cell configuration for X-ray CT measurements.

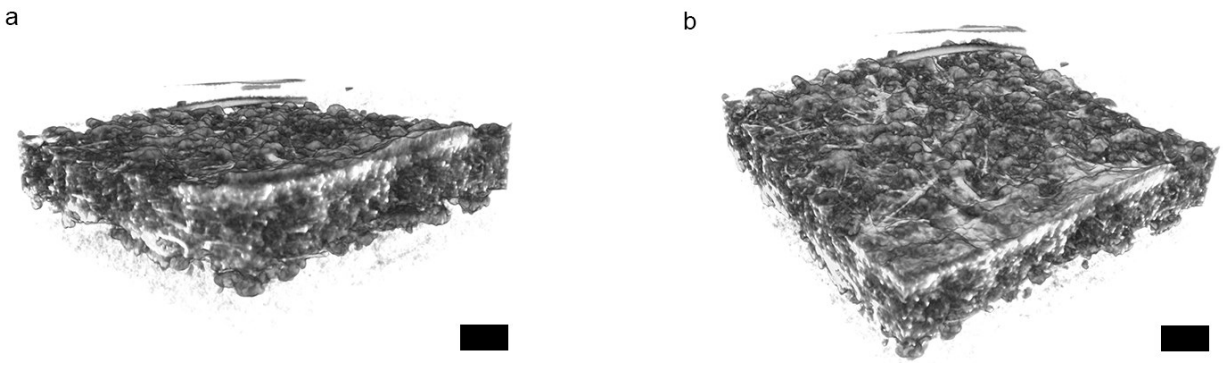

Figure S11. 3D renderings of the separator in the symmetric cells using bare Li after electrochemical cycling by (a) cross-section and (b) top view. The lengths of scale bars are 200 μm.

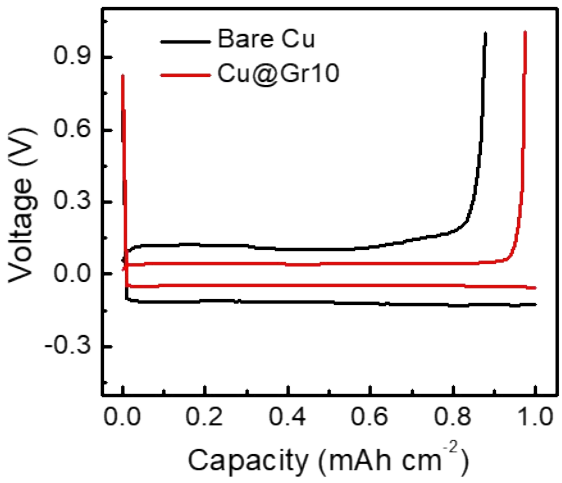

Figure S12. Detailed charge-discharge curves of Li-Cu cells using bare Cu and Cu@Gr10 after 50 cycles at a current of 2 mA cm^{-2}.

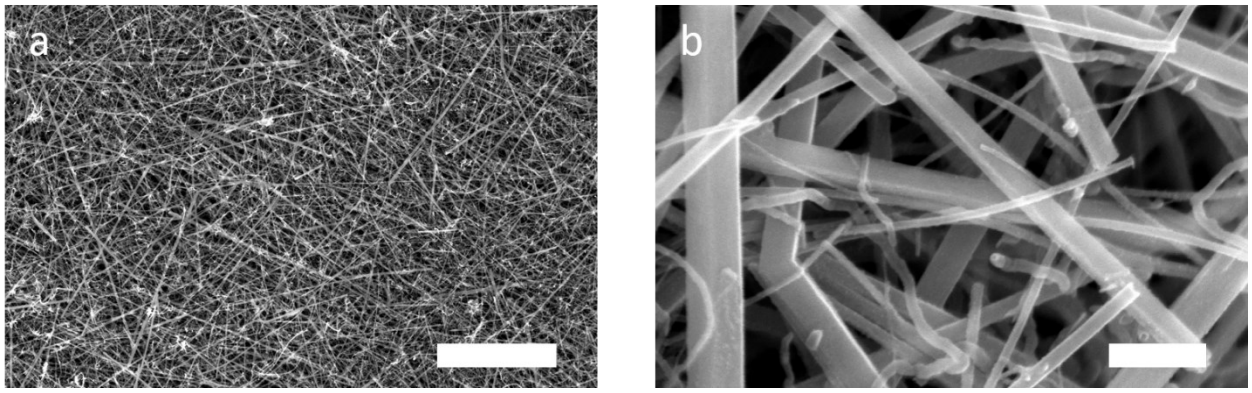

Figure S13. SEM images of Mn_3O_4/CNTs-RuO_2 film for Li-O_2 battery under (a) low-magnification and (b) high-magnification. The lengths of scale bars are 5 μm and 200 nm for (a) and (b), respectively.

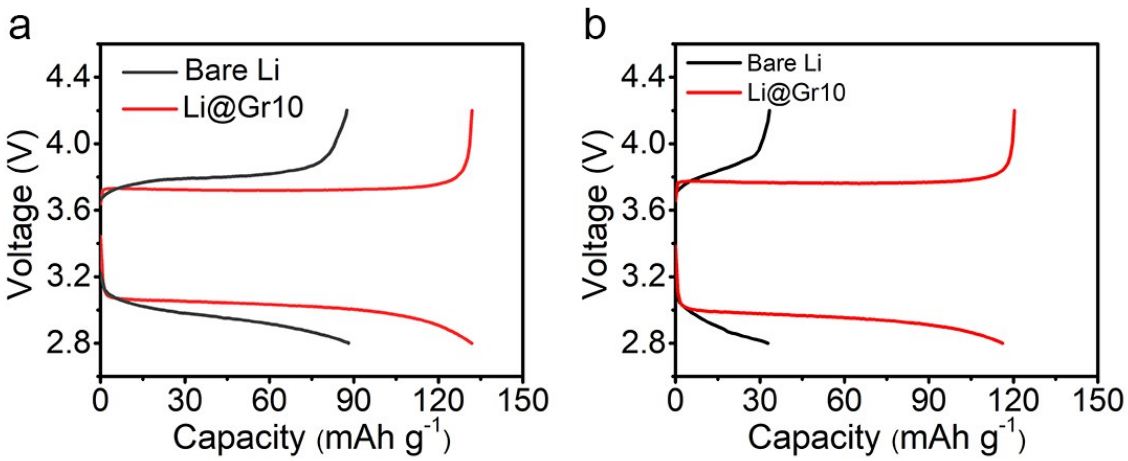

Figure S14. Charge/discharge profiles of Li-LFP batteries using bare Li and Li@Gr10 after (a)200 cycles and (b) 300 cycles.